



Cite this: *Soft Matter*, 2016, 12, 9095

Enhanced mechanical properties of photo-clickable thiol–ene PEG hydrogels through repeated photopolymerization of in-swollen macromer†

C. I. Fiedler,^a E. A. Aisenbrey,^b J. A. Wahlquist,^c C. M. Heveran,^c V. L. Ferguson,^{cde} S. J. Bryant^{bde} and R. R. McLeod^{*ad}

Current hydrogels used for tissue engineering are limited to a single range of mechanical properties within the replicated tissue construct. We show that repeated in-swelling by a single hydrogel pre-cursor solution into an existing polymerized hydrogel followed by photo-exposure increases hydrogel mechanical properties. The process is demonstrated with a photo-clickable thiol–ene hydrogel using a biocompatible precursor solution of poly(ethylene glycol) dithiol and 8-arm poly(ethylene glycol) functionalized with norbornene. The polymer fraction in the precursor solution was varied by 5, 10, and 20 percent by weight and an off-stoichiometric ratio of thiol:ene was used, leaving free enes available for subsequent reaction. Multiple swelling and exposure cycles for the same precursor solution were performed. The compressive modulus increased by a factor between three and ten (formulation dependent), while volume swelling ratio decreased by a factor of two, consistent with increased crosslink density. The modified hydrogels also demonstrate increased toughness by fracturing at compressive forces five times greater than the initial hydrogel. We attribute the increased toughness to subsequent increases in crosslink density created by the repeated photopolymerization of in-swollen macromer. This technique demonstrates the ability to significantly modify hydrogel network properties by exploiting swelling and polymerization processes that can be applied to traditional three-dimensional printing systems to spatially control local mechanical properties.

Received 2nd August 2016,
Accepted 14th October 2016

DOI: 10.1039/c6sm01768a

www.rsc.org/softmatter

Introduction

Hydrogels are the subject of extensive research as tissue scaffolds due to their tunable properties including water content (50–97%), swellability (~ 5 – $15\times$), diffusivity (up to $\sim 100 \mu\text{m}^2 \text{s}^{-1}$) and stiffness (1s to 1000s of kPa).^{1–7} These materials mimic the extracellular matrix of a variety of human tissues, ranging from fat to cartilage.⁸ Hydrogels can also be highly cytocompatible, with cell viability on the order of 95% after weeks of culture.¹

Cartilage repair and regeneration is particularly difficult as the native tissue possesses limited ability to heal. However, a cartilage replacement must bear the physiological loads on the order of $\sim 1000\text{s}$ of N, while simultaneously providing a soft scaffold that is suitable for cells.^{9–13} This dual requirement for spatially controlled tough, high-modulus global behavior that is locally soft and resorbable is challenging to meet with a homogeneous material. A patterned, heterogeneous structure can address this requirement.¹⁴

Stereolithography offers a route to spatially pattern such structures. In all variants of stereolithography, an optical pattern representing a two-dimensional slice of a 3D design hardens a thin layer of resin.^{15,16} As the fabrication is moved away from the light source by a motorized platform, a fresh layer of liquid resin is supplied by the bath surrounding the part. To incorporate a second printing material, the incomplete part must be removed from the bath, washed in a solvent, and placed into a bath of the second macromer resin. This process is slow and wasteful of material.¹⁷ When printing with cell-laden precursor solutions, the solvent wash can lead to cell death.^{17–19} Finally, the high diffusivity of hydrogels causes the

^a Electrical, Computer, and Energy Engineering, University of Colorado Boulder, Boulder, CO 80309, USA. E-mail: mcleod@colorado.edu

^b Chemical and Biological Engineering, University of Colorado Boulder, Boulder, CO 80309, USA. E-mail: sbryant@colorado.edu

^c Mechanical Engineering, University of Colorado Boulder, Boulder, CO 80309, USA. E-mail: virginia.ferguson@colorado.edu

^d Material Science and Engineering, University of Colorado Boulder, Boulder, CO 80309, USA

^e BioFrontiers Institute, University of Colorado, Boulder, CO 80309, USA

† Electronic supplementary information (ESI) available: PEG–norbornene ¹H NMR spectra, precursor solution control experiment, equilibrium swelling experiment, best fit polynomial regression statistics. See DOI: 10.1039/c6sm01768a

subsequent macromer solutions to rapidly penetrate the existing solidified gel, making it difficult to pattern distinct features.

Previous research by DeForest *et al.*²⁰ and Marklein *et al.*²¹ exploited this rapid diffusion of molecules into a previously polymerized hydrogel to spatially pattern different chemical cues that control stem cell differentiation, by in-diffusing functionalized macromer solutions and locally photopolymerizing. Similarly, Ducrot *et al.*²² and Gong *et al.*^{23,24} demonstrated modification of an existing polymer network by swelling the original matrix with a second precursor solution, which was then polymerized, forming a double network (DN) hydrogel. While these techniques demonstrated that macromer transport followed by photopolymerization can selectively modify properties of biologically relevant hydrogels, the use of multiple macromer formulations is inherently difficult for stereolithography, as described.

To overcome these challenges, transport of the original macromer solution into the printed gel can be exploited to obtain large variations in mechanical properties using only a single macromer solution, avoiding removal from the bath and solvent wash. Specifically, precursor solution of the same formulation is allowed to swell into an existing polymerized matrix and is selectively polymerized, locally modifying the hydrogel properties.²⁴ Exploiting the rapid transport inherent to hydrogels and using a single precursor solution to produce a mechanically diverse 3D structure enables the large range of mechanical properties required for cartilage replacement to be efficiently fabricated in a stereolithographic 3D printer.

This study investigates the range of mechanical properties a single precursor solution can produce by cyclically in-swelling fresh precursor solution followed by photo-exposing the swollen gel ("swelling + exposure" or SE cycle), as illustrated in Fig. 1.^{21–23} We employ a cytocompatible photo-clickable poly(ethylene glycol) macromer solution to demonstrate this technique, which consists of PEG-dithiol and 8-arm PEG-norbornene.^{25–27} We chose three cytocompatible precursor solution formulations of 5, 10, and 20 wt% macromer concentration in phosphate buffered saline

(PBS) to investigate, each of which underwent 10 SE cycles.^{13,25} The process was terminated at 10 cycles based on the observation that properties changed rapidly in the first several cycles and much more slowly by cycle 10. Comparing the gels that underwent zero SE cycles (single network gels) to those that underwent multiple SE cycles, we demonstrate that hydrogel mechanical properties can be increased by more than an order of magnitude using this technique, *e.g.*, compressive moduli increase from 10s kPa to 100s kPa. By characterizing the range of mechanical properties in bulk hydrogel, this work can be extended and implemented into a 3D printing system to spatially photo-pattern mechanical properties using a single material, as shown herein.

Experimental procedure

Materials

Poly(ethylene glycol)dithiol (PEG-dithiol) (Sigma Aldrich, MW 1000 Da), poly(ethylene glycol)thiol(tripentaerythritol) (JenKem USA, 8ARM-PEG-SH, MW 10 000 Da), and lithium phenyl-2,4,6-trimethylbenzoylphosphinate (LAP) (Colorado Photopolymer Solutions) were used as received. 5-Norbornene-2-carboxylic acid (NB) (Sigma Aldrich) was conjugated to poly(ethylene glycol)amine (PEG-NH₂) (JenKem USA, 8 arm PEG amine, HCl salt, MW 10 000 Da) at room temperature (RT) under an argon purge to produce poly(ethylene glycol)norbornene (PEG-NB).¹³ This was done by dissolving PEG-NH₂ (10 g) in dimethylformamide (DMF) (15 mL) and dichloromethane at 1:1 ratio to which the solution containing 4 molar excess NB (4.42 g), 2 molar excess 2-(1*H*-7-azabenzotriazol-1-yl)-1,1,3,3-tetramethyl uronium hexafluorophosphate methanaminium (HATU, AKSci) (9.12 g), and 2 molar excess *N,N*-diisopropylethylamine (DIEA, Sigma) (6.2 g) was reacted with for 48 hours. The solution was precipitated in diethyl ether, dialyzed four times with diH₂O over two days, and lyophilized. The resulting 8-arm PEG-NB product conjugation of 99% (percentage of NB conjugated PEG arms), referred to herein as PEG-NB. The degree of norbornene conjugation was determined by ¹H NMR (Bruker AV-III 400) by comparing the area under the peak for the allylic hydrogen closest to the norbornene bridged cyclic hydrocarbon group (resonance from ~3.1 to 3.2 ppm) to the area under the peak for the methyl groups in the PEG backbone (resonance from ~3.4 to 3.85 ppm), see ESI 1† for ¹H NMR spectrum. Macromers were dissolved in phosphate-buffered saline (PBS) (OmniPur, Calbiochem).

Sample preparation

PEG-NB and PEG-dithiol (at 0.25:1, 0.5:1, 0.75:1, and 1:1 thiol:ene ratios) were combined with cytocompatible UV photoinitiator LAP²⁵ at 0.05 wt% in PBS at three precursor solution concentrations of 5, 10, and 20 wt% of total macromer. First PEG-NB was dissolved into PBS for 10 h, PEG-dithiol and LAP were then added immediately before use to minimize the formation of disulfide bridges within the solution. A volume of 20 μL precursor solution was then added to 3 mm diameter by 5 mm cylindrical molds and

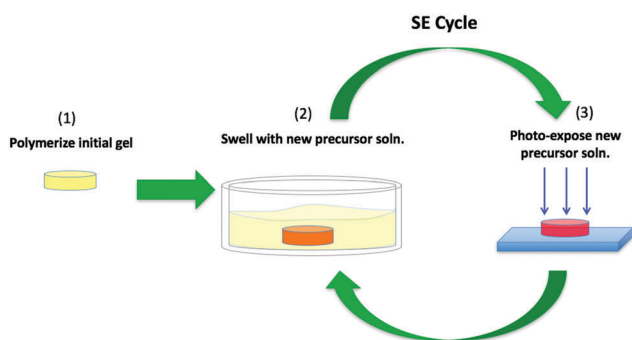


Fig. 1 (1) The initial precursor solution is placed into a cylindrical mold and photopolymerized into a hydrogel. (2) The hydrogel is then placed into a bath containing the same macromer and photoinitiator concentrations as were used to form the initial gel and swollen to equilibrium. (3) The swollen gel is removed and immediately polymerized using the same exposure conditions as step 1. Steps 2–3 encompass a single SE cycle, which is repeated up to 10 times.

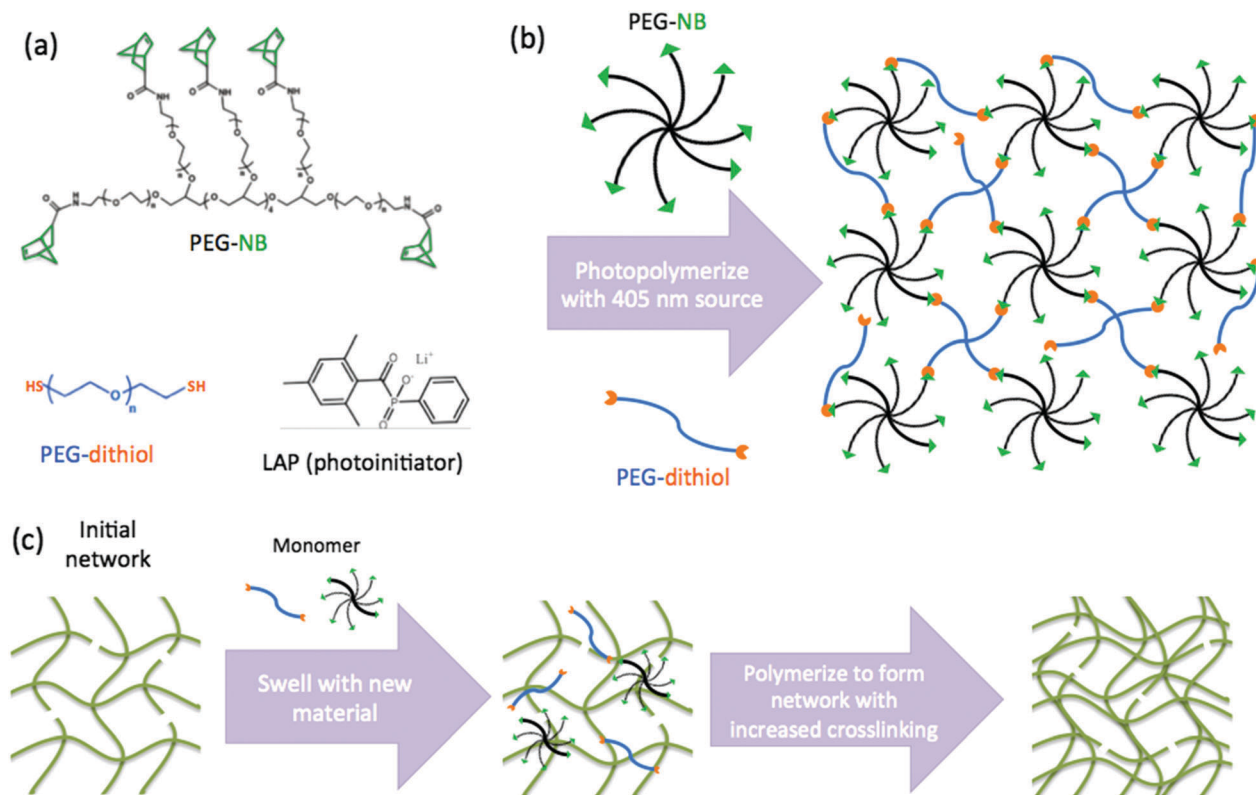


Fig. 2 (a) The chemical structure of the precursor solution components, where the green and orange regions indicate the functional groups norbornene and thiol, respectively. (b) An illustration of initial network formation showing remaining functional groups after polymerization. (c) A cartoon depicting the network transformation after a single SE cycle.

photopolymerized with a uniform intensity 405 nm illumination (OmniCure S1000) at RT for 6 minutes (13 mW cm^{-2}) to form a cylindrical hydrogel, with the diameter ~ 3 mm and height ~ 2 mm. Because the hydrogels are formed at a high solvent concentration and off stoichiometry, unreacted 'enes' and any unreacted thiols are free to react with new precursor solution, as shown in Fig. 2.

To modify the characteristics of the existing polymer network, the gel was then placed into a fresh bath of precursor solution containing the same concentrations of macromer and photoinitiator as used to form the original gel. The precursor solution bath volume was maintained at 15 times greater than the gel volume to prevent significant concentration dilution of the bath during swelling. Each hydrogel was swollen to approximate equilibrium at RT by leaving it in the bath for a time determined by a series of swelling experiments, as described below and ESI 2.†

To ensure homogeneous concentration of the precursor solution bath throughout swelling, it was placed onto an orbital shaker at an oscillation speed of 90 rpm. The gel was then removed, gently dried (removing only liquid remnants on surface of gel), and immediately polymerized with a 405 nm exposure source.

The above process was repeated 10 times, $n = 3-4$ trials per cycle. Each gel was then placed into a bath of deionized (DI) water and swollen to equilibrium for 24 hours. DI water

replaced the previously used PBS to remove the salts from the dried gel mass, and all swelling measurements were taken at this time.

Characterization

Mechanical properties. Unconfined compression tests were performed using a Material Testing System (MTS) Insight 2 (MTS Systems Corporation). Two different capacity (5 N and 250 N) load cells were used to encompass the varying maximum loads produced by compressing each of the equilibrium swollen, $3 \text{ mm} \times 2 \text{ mm}$ cylindrical gel samples (*i.e.*, the 250 N load cell was required to test 10 wt% gels from SE cycles 4–10 and all 20 wt% samples). Stress–strain tests were all run to failure. The duration of each compression test was under 5 minutes, a sufficiently short time to neglect the effects of evaporation.

The compressive modulus (hereafter termed 'modulus') was found using engineering stress–strain curves taken for equilibrium-swollen hydrogels in DI water (Fig. 3). Hydrogel toughness was determined by compressing each gel at a rate of 0.5 mm min^{-1} until failure (*i.e.*, the point at which the gel experienced fracture as indicated by a severe drop in stress) and then integrating the region under the stress–strain curve to obtain toughness prior to failure. The ultimate strength is the highest stress attained before failure. It should be noted that all stress and strain values presented herein are based on preloaded sample dimensions using infinitesimal strain assumptions.²⁸

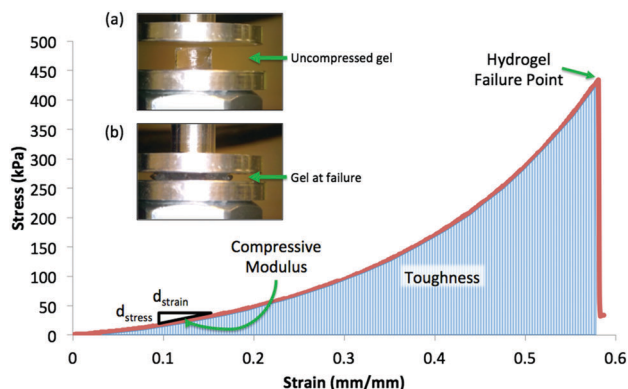


Fig. 3 Stress–strain curve illustrating the hydrogel behavior under compressive loading and subsequent failure where the slope of the curve at 15% strain was used to determine the engineering compressive modulus, and the shaded region indicates the toughness. (inset) (a) and (b) Show images of a single hydrogel sample before compression and at compressive failure known as ultimate compressive stress, respectively.

The hydrogel equilibrium volumetric swelling ratio, Q , was determined by

$$Q = 1 + \frac{\rho_p}{\rho_s} \left(\frac{M_s}{M_d} - 1 \right), \quad (1)$$

where M_s is the equilibrium DI swollen mass of each gel, M_d is the polymer mass after lyophilization, ρ_p is the polymer density assumed to be 1.08 mg mL^{-1} , and ρ_s is the density of water (1 g mL^{-1}).^{26,28} From equilibrium volumetric swelling ratio, the polymer volume fraction is defined by³⁴

$$\phi = Q^{-1}, \quad (2)$$

We estimated crosslink density, ρ_x and the polymer–solvent interaction parameter, χ_{12} using a self-learning model described by Akalp *et al.*²⁹ This model uses the experimentally determined parameters of polymer volume fraction (*i.e.*, ϕ) and the modulus of the fully swollen as inputs and solves for ρ_x and χ_{12} by combining Flory–Rehner theory with theories of mixture and poroelasticity.^{30–33} The model assumes isotropic swelling and uses a modified version of Flory–Rehner theory that neglects the contribution of chain ends. These assumptions are reasonable for unconstrained swelling conditions and have been shown to predict swelling and modulus of similar PEG hydrogels.²⁹

The linear deformation of a hydrogel network, assuming isotropic swelling, is described by $Q^{1/3}$.³⁵ To understand the impact of in-swelling on the level of polymer chain stretching at each SE cycle, the ratio of linear deformation of the hydrogel at equilibrium ($Q_{n,f}^{1/3}$) to the linear deformation of hydrogel immediately after the gel is formed but before swelling ($Q_{n,i}^{1/3}$) was evaluated for cycle n . This ratio is defined in terms of ϕ by³⁴

$$\lambda_n = \left(\frac{\phi_{n,i}}{\phi_{n,f}} \right)^{1/3}. \quad (3)$$

Statistical analysis

Polynomial regression, a special case of multiple linear regression, was performed for each mechanical property response (modulus, toughness, swelling ratio) in models including SE cycle, SE², and SE³. For each dependent variable, the models were constructed and compared for each combination of linear, quadratic, and cubic orders of SE. Model selection favored overall model significance ($p < 0.05$), and high R^2 (adjusted) (ESI 3†). For several responses, log transformation of the dependent variable was necessary to satisfy model assumptions of normally distributed residuals and unstructured residuals *versus* model fits. Simple linear regression was used to evaluate the relationship between toughness and modulus where model assumptions were satisfied. Two-factor ANOVA considered the effect of hydrogel composition (5, 10, 20 wt%) and bath composition (with or without photoinitiator) on mechanical properties. For all analyses, alpha was set *a priori* at 0.05. All statistics were performed with Minitab (v.17).

Photopatterned hydrogel

Photopatterning was performed using a projection stereolithography system. The system employs a Mightex Polygon 400 Digital Spatial Illuminator (DSI), which contains a 405 nm light source and a digital micromirror device (DMD), to produce a pattern that we image onto to the hydrogel sample plane. To image the photopatterned samples, confocal fluorescence microscopy was used after each gel was submerged in DI water until swollen to equilibrium and all excess, unreacted precursor solution was removed.

Results and discussion

Preparation of PEG hydrogels

To enable new precursor solution to react with the existing network, an off-stoichiometric ratio of thiol to ‘ene’ was used to ensure ‘ene’ groups remained unreacted after the initial network polymerization. We varied the thiol to ‘ene’ ratios from 0.25:1 to 1:1 at increments of 0.25 and characterized their mechanical and swelling properties and crosslink density, as shown in Fig. 4. We chose the 0.5:1 ratio because it exhibited structural stability while leaving at least half of the initial ‘ene’ groups unreacted after the initial polymerization.

As a control experiment to verify that mechanical properties did not change in a single network gel by simply providing additional photoinitiator, a solution of 0.05 wt% LAP in PBS was swelled into the initial single network hydrogels and exposed. As shown in ESI 4,† no significant change in hydrogel properties was observed. This confirms that any change in mechanical properties, as a function of SE cycle, are the result of polymerization of new macromer.

To ensure that the length of time in the precursor solution bath was sufficiently long to allow each gel to approach equilibrium, gels of each formulation were placed into a bath of precursor solution and incrementally removed to observe swollen mass as a function of time in the bath. Soak times of 6, 6, and 12 hours for the 5, 10, and 20 wt% gels, respectively, were

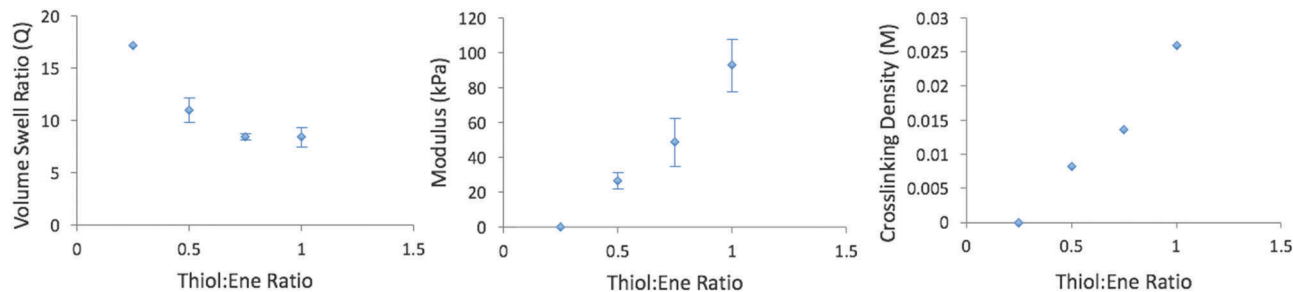


Fig. 4 The macroscopic properties of photo-clickable PEG hydrogels that were formed by varying the thiol:ene ratio from 0.25:1 to 1:1 using a precursor solution of 10 wt% macromer and 0.05 wt% LAP. The macroscopic properties are volumetric swelling ratio, Q , modulus, and crosslinking density, where $n = 3-4$ and the vertical error bars (blue) indicate the standard deviation of a given sample set.

determined for each SE cycle when the swollen mass had leveled off and no continued mass gain observed, which occurred after 5 hours of submersion for each formulation (ESI 2a†).

To confirm experimentally that new macromers were transported into the hydrogel at each SE cycle, the dry polymer mass was obtained after each cycle, but before swelling, following lyophilization. For all formulations, the dry mass increased with SE cycle, demonstrating the in-swelling of new precursor solution into the gels (ESI 2b–d†). We note that for the 5 wt% 0.5:1 hydrogels, the PBS salts were not diffused out from the hydrogel and contributed to and enhanced initial dry mass observed. To correct for this, the mass associated with the PBS salts that remain after lyophilization was determined and then subtracted from the dry mass.

The gels were designed with an off-stoichiometric ratio, leaving approximately 50% of the norbornene functional groups remaining after polymerization. However, non-idealities can leave behind unreacted thiols as well as norbornenes. To determine whether the PEG-NB macromer reacts significantly with free thiols, and thus contributes to the initial network, swelling of solely PEG-NB and photoinitiator in PBS into the single network hydrogel followed by light exposure was investigated. No significant changes were observed in the modulus when hydrogels of 5, 10, and 20 wt% macromer with 0.5:1 thiol to ene ratios were prepared and swollen with fresh precursor solution of 0.05 wt% LAP in PBS with solely the PEG-NB macromer. This observation suggests that the concentration of free thiols in the initial network is low. However, diffusion of the PEG-NB macromer will be more limited due to its size and thus its concentration may be low.³⁵ Consequently, any reactions to the initial network may not, on its own, contribute significantly to the macroscopic properties. However, swelling the hydrogels with PEG-dithiol and photoinitiator in PBS led to increases in the compressive modulus by a factor of two (ESI 5†). It is important to note that each gel was submerged in their respective precursor solution until equilibrium swelling was reached.

The necessity for an off-stoichiometric ratio of ‘enes’ to thiols was first probed by using the 5 wt% precursor solution, but with a 1:1 stoichiometric ratio between functional groups. This test was subject to 6 SE cycles as previously described. A positive, linear relationship between modulus and SE cycle as well as crosslink density and SE cycle was found ($p < 0.0001$

and $p = 0.014$, respectively), while the swelling ratio to SE cycle exhibited a negative, linear relationship ($p < 0.0001$) (Fig. 5a–c). The increase in modulus and decrease in swelling observed here is attributed to the presence unreacted thiol and ene functional groups that result from inefficiencies in crosslinking due to the high solvent concentration. The change in hydrogel properties was modest and even with multiple cycles, no relationship between toughness and SE cycle was found ($p = 0.77$) (Fig. 5d). This result corresponds with trends in elastic modulus data from the literature where the introduction of more precursor solution and subsequent polymerization to an already formed network with no accessible reactive groups, negligibly contributes to increased stiffness.^{21,36} Based on these results, an off-stoichiometric ratio precursor solution was selected for subsequent experiments to investigate changes in macroscopic properties with SE cycle.

Characterization of enhanced PEG hydrogels

This study demonstrates that repeated precursor in-swelling and exposure cycles affect both the modulus and the toughness of PEG hydrogels. We observed an order of magnitude increase in the modulus after 2–4 cycles for all precursor solution formulations (Fig. 6). We hypothesize that during these cycles, the remaining ‘enes’ in the first network further react creating a more densely crosslinked network, evident by the increase in modulus. Because we observed greater increase in modulus after a single SE cycle than when solely swollen with a PEG-dithiol solution (ESI 5†), the presence of PEG-norbornene in the in-swollen precursor solution contributes to the observed increased modulus. With each cycle, ‘enes’ and thiols are consumed, but new pendant free ‘enes’ and thiols are introduced leading to further increases in the crosslink density and subsequent modulus. However, beyond approximately 3 SE cycles, the modulus reached a plateau.

Concomitant with the increased modulus, we observed an increase in toughness of the hydrogels as they underwent up to ~2 SE cycles. The failure point was noted by a sharp decrease in the stress–strain curve corresponding to irreversible, inelastic damage with visibly fractured gels. The gel toughness increased for all formulations, for example by a factor of 4 for the 20 wt%. For the responses of modulus and toughness, models with quadratic and cubic terms of SE achieved the best fit. These models confirm

1:1 Stoichiometric Ratio Precursor Solution Formulation

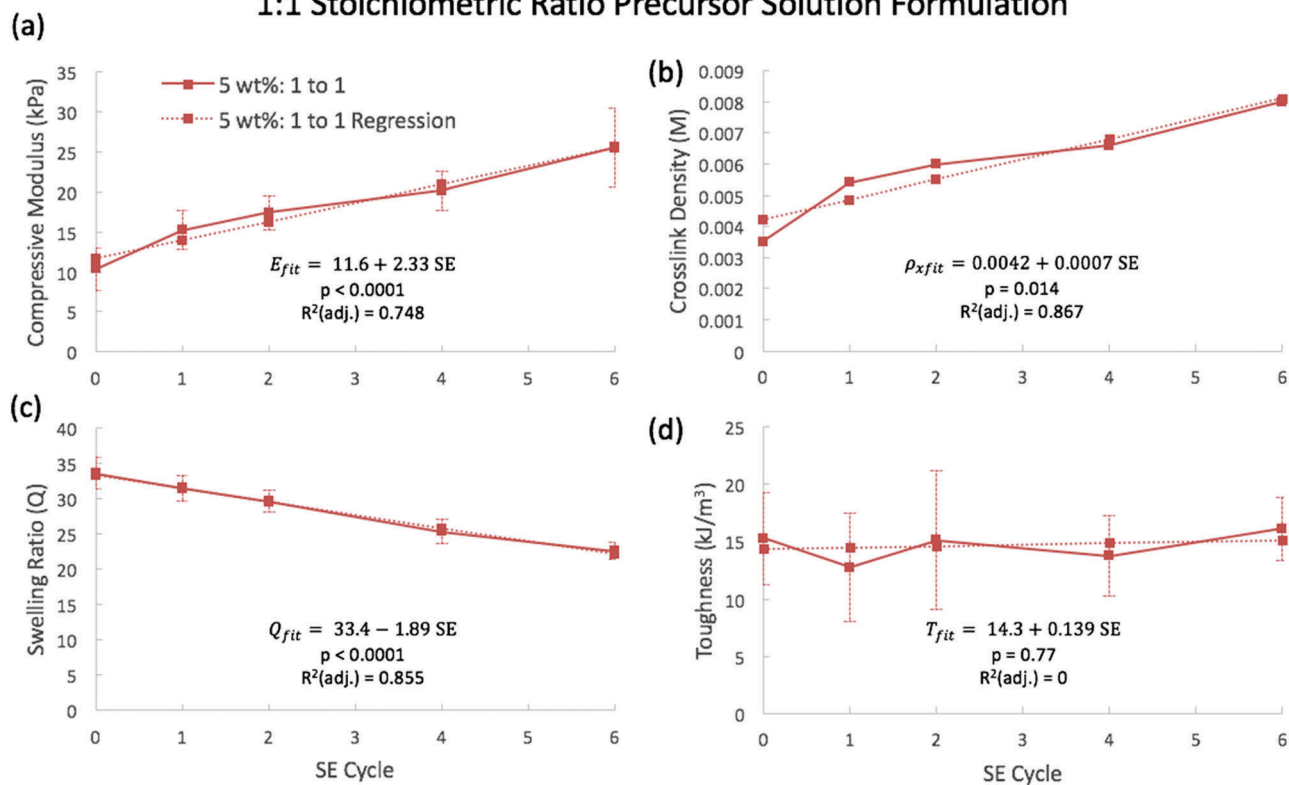


Fig. 5 (a) Changing thiol to 'ene' ratio from 0.5 : 1 to 1 : 1, modulus and (b) crosslink density linearly increase for all SE cycles ($p < 0.0001$ and $p = 0.014$, respectively). (c) The swelling ratio conversely decreased linearly for all SE cycles. (d) No significant relationship between toughness and SE cycle was visible after repeating 6 SE cycles ($p = 0.77$). The solid lines represent experimental data while the dotted represents the best-fit regression model.

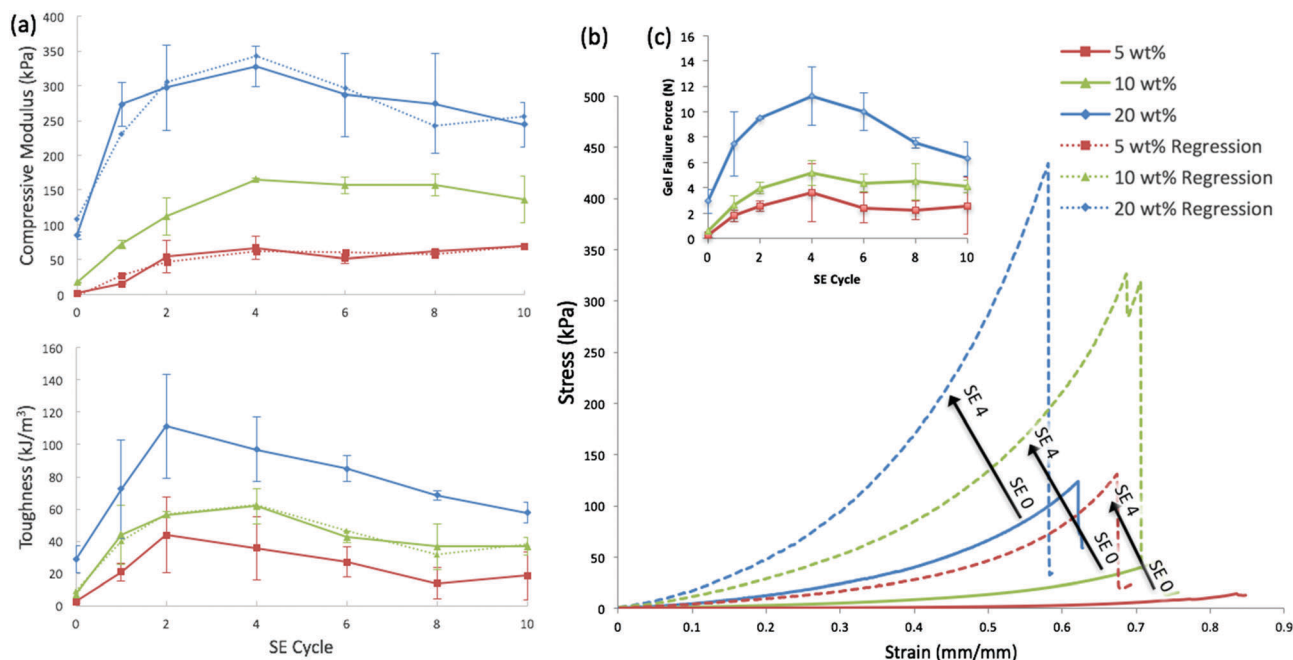


Fig. 6 (a) For all precursor solution formulations (5 (red), 10 (green), and 20 (blue) macromer wt%), the modulus and toughness increases until a plateau or decrease is reached at 2–4 SE cycles, polynomial regression confirms that mechanical property data are best fit with a model including SE, SE², and SE³. The shape of the most appropriate model confirms the presence of maxima in mechanical properties between 2–4 SE. For the full regression fits, p -values, and R^2 values see ESI 2.† (b) Shows the stress–strain curves until failure for each PS formulation at cycles 0 (solid line) and 4 (dashed line), where (c, inset) displays the ultimate strength as a function of SE cycle. All data are presented as mean with standard deviation as error bars for $n = 3–4$.

the presence of a maxima (2–4 cycles), after which mechanical properties decreased with additional cycles.

For each precursor solution formulation, the equilibrium volumetric swelling ratio, Q , (Fig. 7a) decreased as a function of SE cycle and reached a plateau after 3–4 SE cycles. As shown in Fig. 7b, the crosslink density also follows this trend, which increased as a function of SE cycle until approximately 2–4 SE cycles, where the crosslink density reached a plateau (5 and 10 wt% gels) or decreased (20 wt% gels).

Two hypotheses for the plateaus observed in the modulus, Q , and crosslink density are proposed. First, the macromers were not given adequate time to be transported into the gel once the gel had undergone multiple SE cycles. However, long times (~ 6 –12 hours) were employed and the dry and swollen polymer masses (ESI 2b†) increased with each SE cycle, suggesting that transport was not limited. Alternately, a complex, multi-network system may be forming. In support of this hypothesis, the dry polymer and swollen masses continued to increase beyond cycles 3–4 even though there were no longer any appreciable changes in mechanical or swelling properties. These data confirm that macromer is still being transported into the hydrogel and subsequently reacting and thus point to the formation of interpenetrating networks. It is interesting, though, that the behavior the hydrogels formed herein differ substantially from typical double networks, which utilize two distinctly different materials, that exhibit an increase in toughness with the addition of the second material, while modulus remains approximately constant.^{22–24,36} A linear regression analysis of toughness to modulus shows a positive correlation ($p < 0.0001$, $R^2(\text{adj.}) = 0.676$), indicating that increase in modulus corresponds with increase in toughness in hydrogels fabricated *via* multiple SE cycles (Fig. 8). This finding is consistent with single network hydrogels where increasing crosslinking increases both modulus

and toughness. These data thus suggest that in the initial SE cycles, the degree of crosslinking in the initial network increases leading to the combined increased in modulus and toughness. However, the plateau in properties at SE cycles of ~ 2 –4 suggest that the bonds in this initial network dominates the mechanical properties at later SE (*i.e.*, $> \sim 2$ –4) cycles.

To further understand how the network changes with increasing SE cycle, we calculated the linear deformation, λ , which is a measure of polymer chain stretching within the hydrogel relative to its dry state (Fig. 9a). As expected, the polymer chains in the initial network (*i.e.*, SE = 0) are more stretched in the 5 wt% (*i.e.*, low crosslinked) formulation compared to the more tightly crosslinked 10 and 20 wt% formulations. With increasing SE cycles up to \sim SE 2, additional crosslinks are introduced into the initial network and overall the polymer chains do not stretch to the same extent as in the previous SE cycle. It should be noted that with each SE cycle, a distribution of polymer chains exists in different stretched states; however, λ represents the average of all chains. At SE $> \sim 2$, the linear deformation no longer changes with increasing SE cycle for each formulation. Interestingly, however, the percent polymer mass continues to increase (*e.g.*, by 70% from SE 2 to SE 10 for the 5 wt% formulation). Our data indicate that additional crosslinks are being introduced into the initial network (b/w SE 2 and \sim SE 4) as evidence by an increase in modulus and that an interpenetrating network(s) is like forming in subsequent SE cycles as indicated by the increased weight gain. Since λ represents an average of chain stretching, it is reasonable to postulate that the chains in the initial network continue to be stretched with each SE cycle, but the new polymer chains that are introduced are less stretched. This statement is supported by data in Fig. 9b, which describes the level of polymer stretching at equilibrium relative to the prepared state

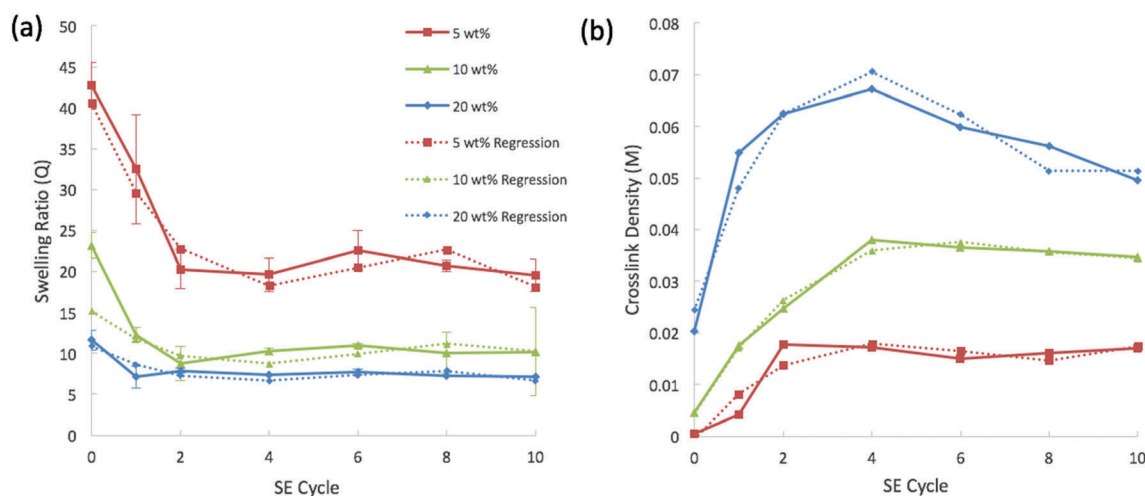


Fig. 7 (a) For all precursor solution formulations, a sharp decrease in the equilibrium volume swelling ratio, where Q was normalized to the dry mass of the hydrogels that underwent 0 SE cycles to account for sample variation. (b) The crosslink density experienced a similar trend to the mechanical properties, increasing until 2–4 cycles and then reaching a plateau. Polynomial regression analyses of Q versus linear and higher-order expressions of SE reveal that the best model fit is achieved with inclusion of SE, SE², and SE³ terms. The best fitting model shows a maximum in Q between 2–4 SE cycles with $p < 0.05$ for all sample sets (ESI 2†). All data are presented as mean with standard deviation as error bars for $n = 3$ –4 except crosslink density, which was determined using all technical repeats ($n = 3$ –4) per condition in a self-learning algorithm.

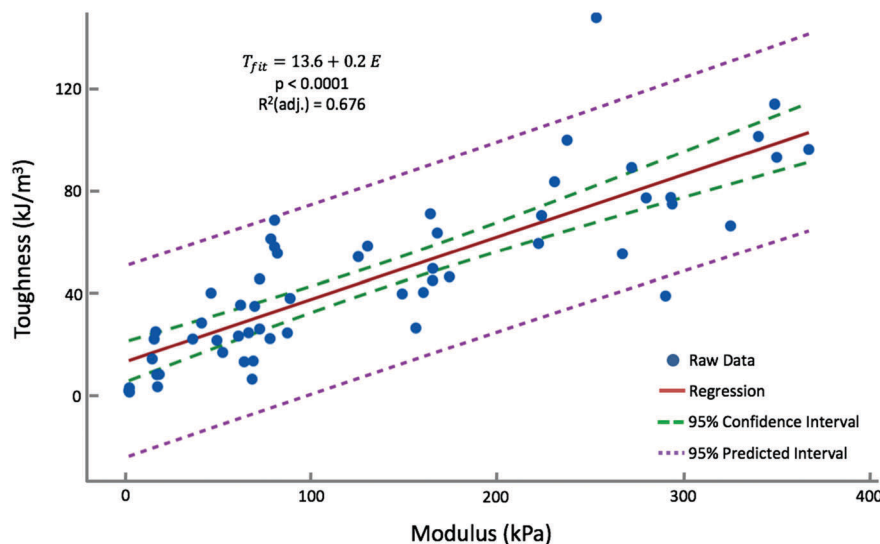


Fig. 8 Linear regression analysis (red solid line) confirming the positive relationship between increased modulus (E) and toughness (T) of SE cycle fabricated hydrogels with $p < 0.0001$ and $R^2(\text{adjusted}) = 0.6759$. The 95% confidence (green dashed line) and predicted (purple dotted line) intervals are also plotted to highlight the model-to-data fit.

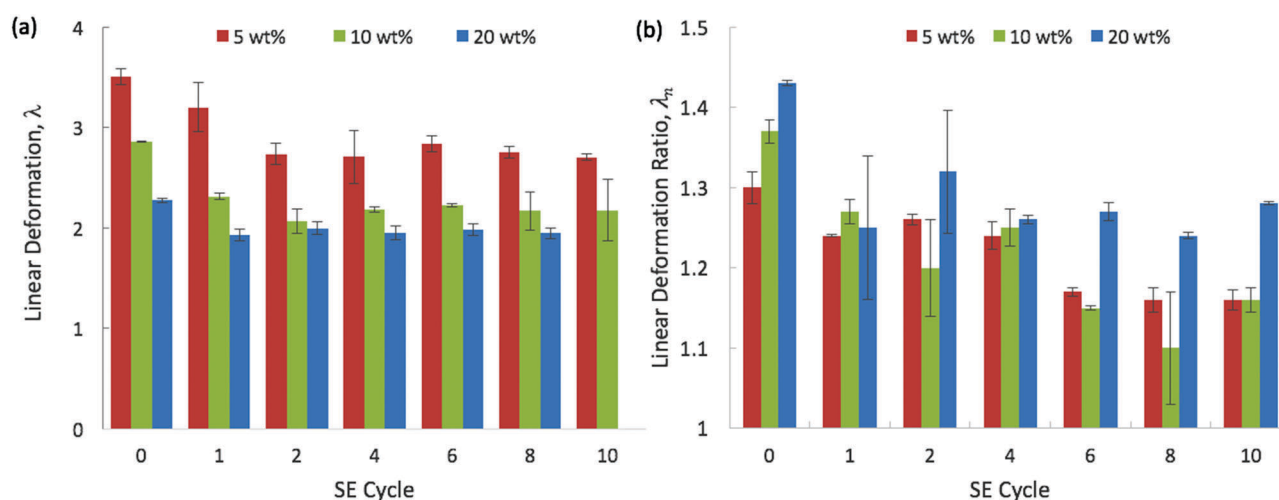


Fig. 9 (a) Linear deformation decreased a function of SE cycle, ($p < 0.02$ for all formulations). (b) The linear deformation ratio comparing the linear deformation of the swollen network to that of the network immediately following polymerization also significantly decreases as a function of cycle ($p < 0.0001$ for 5 and 20 wt% gels).

(*i.e.*, before swelling to equilibrium) for each SE cycle. Notably for the 5 and 10 wt% formulations, this λ_n ratio decreases with increasing SE through SE 10. This further supports that the new polymers introduced are in a much reduced stretched state. For λ to stay the same, the chains in the initial network, must then become increasingly stretched.

Collectively, the mechanical and swelling behaviour of PEG hydrogels formed *via* multiple SE cycles are largely dominated by the initial network. With the presence of free reactive groups after hydrogel formation, the initial network continues to grow with subsequent cycles. This led to a higher modulus and subsequent higher toughness due to the presence of more crosslinks. However, as the chains in the initial network become more stretched with subsequent cycles, they require

less force to break and thus dissipate lower energy during failure.^{22,37} Indeed, we observed a decrease in toughness with increasing SE cycles from ~ 2 –4 to 10. While interpenetrating networks are likely present, our data suggest that they are at a sufficiently low crosslink density and thus unable to contribute to the mechanical properties and notably toughness. Additional studies, however, are required to experimentally verify the exact nature of the networks formed using this SE approach.

We demonstrate the ability to photopattern using this SE approach with $\sim 10 \mu\text{m}$ resolution and minimum feature size using a projection stereolithography system. An initial network was formed off-stoichiometry as before, which was then in-swollen with a fresh precursor solution containing fluorophore-attached thiol (AlexaFluor 546, 1 : 5000, fluorophore : thiol). The hydrogel

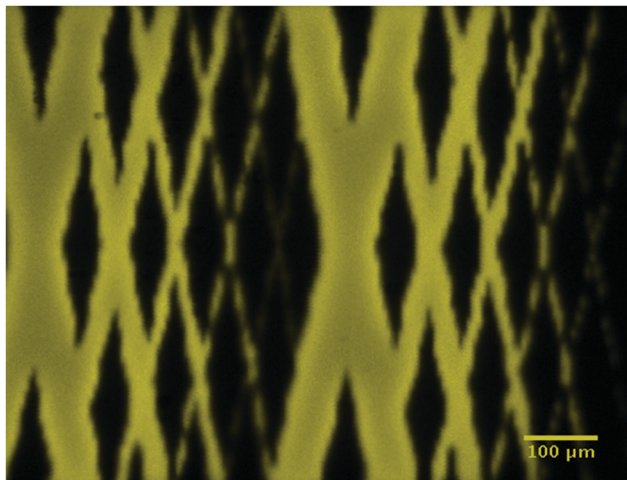


Fig. 10 Confocal microscopy image of photopolymerized resolution test pattern printed into a single network hydrogel matrix, effectively producing a network representative of 1 SE cycle in the newly exposed, yellow region and 0 SE cycles is represented by the dark regions.

was exposed to a resolution test pattern to initiate a secondary polymerization within the exposed regions. The resulting hydrogel was imaged using confocal microscopy (Fig. 10). In doing so, we demonstrate the ability to locally photopattern hydrogels using this new concept of SE cycles.

Conclusion

Using a single precursor solution, the modulus and toughness of PEG hydrogels was shown to increase by 5–10 \times by in-swelling and polymerizing new macromer into an existing polymer network. Our data point to the initial network that forms during the first few SE cycles as dominating the macroscopic behavior of the hydrogel. This approach offers an elegant solution to spatially patterning mechanical properties in a biocompatible hydrogel. Because substantial material property changes can be achieved after 2–4 SE cycles, the small length scales of 3D printing (10s of μm) enable fabrication of mechanically diverse structures. Though the hydrogels tested here were not designed to bear forces sustained by native articular cartilage tissue, we offer a method to substantially increase the modulus and toughness of biocompatible hydrogels for tissue engineering applications.

Acknowledgements

This research was supported by the National Science Foundation Graduate Research Fellowship (DGE 1144083 to CIF, DGE 2012137234 to EAA), NSF 0847390, and NIH SBIR 1R43MH102946-01. Research reported in this publication was also supported by the National Institute of Arthritis and Musculoskeletal and Skin Diseases of the National Institutes of Health under Award Number NIH 1R01AR069060. The content is solely the responsibility of the authors and does not necessarily represent the official views of the National Institutes of Health.

References

- 1 S. J. Bryant, K. S. Anseth, D. A. Lee and D. L. Bader, *J. Orthop. Res.*, 2004, **22**, 1143–1149.
- 2 Y. Luo and M. S. Shoichet, *Nat. Mater.*, 2004, 249–253.
- 3 A. J. Engler, S. Sen, H. L. Sweeney and D. E. Discher, *Cell*, 2006, 677–689.
- 4 R. Farley, S. Halachera, J. Bramhill and B. R. Saunders, *Polym. Chem.*, 2015, 2512–2522.
- 5 Q. Chen, H. Chen, L. Zhu and J. Zheng, *J. Mater. Chem. B*, 2015, 3654–3676.
- 6 N. A. Peppas, *Curr. Opin. Colloid Interface Sci.*, 1997, **2**, 531–537.
- 7 S. Limem and P. Calvert, *J. Mater. Chem. B*, 2015, **3**, 4569–4578.
- 8 R. Langer and J. P. Vicanti, *Science*, 1993, **14**, 920–926.
- 9 G. Bergman, G. Deuretzbacher, M. Heller, F. Graichen, A. Rohlmann, J. Strauss and G. N. Duda, *J. Biomech.*, 2001, **34**, 859–871.
- 10 D. D. D’Lima, B. J. Fregly, S. Patil, N. Steklov and C. W. Cowell Jr., *Proc. Inst. Mech. Eng., Part H*, 2012, **226**, 95–102.
- 11 G. Bergman, G. Deuretzbacher, M. Heller, F. Graichen, A. Rohlmann, J. Strauss and G. N. Duda, *J. Biomech.*, 2001, **34**, 859–871.
- 12 L. D. Amer and S. J. Bryant, *Ann. Biomed. Eng.*, 2016, **44**(6), 1959–1969.
- 13 J. J. Roberts and S. J. Bryant, *Biomaterials*, 2013, **34**(38), 9969–9979.
- 14 K. S. Allan, R. M. Pilliar, J. Wang, M. D. Grynypas and R. A. Kandel, *Tissue Eng.*, 2007, **13**, 167–177.
- 15 F. P. W. Melchels, J. Feijen and D. W. Grijma, *Biomaterials*, 2010, **31**, 6121–6130.
- 16 A. C. Urness, E. D. Moore, K. K. Kamysiak, M. C. Cole and R. R. McLeod, *Light: Sci. Appl.*, 2013, **2**, e56.
- 17 V. Chan, P. Zorlutuna, J. Jeong, H. Kong and R. Bashir, *Lab Chip*, 2010, **10**, 2062–2070.
- 18 M. Guvendiren, J. Molde, R. M. D. Soares and J. Kohn, *ACS Biomater. Sci. Eng.*, 2016, **2**, 1679–1693.
- 19 S. J. Bryant, C. R. Nuttelman and K. S. Anseth, *Biomed. Sci. Instrum.*, 1999, **35**, 309–314.
- 20 C. DeForest, B. Polizzotti and K. S. Anseth, *Nat. Mater.*, 2009, **8**, 659–664.
- 21 R. A. Marklein and J. A. Burdick, *Soft Matter*, 2010, **6**, 136–143.
- 22 E. Ducrot, Y. Chen, M. Butlers, R. P. Sijbesma and C. Creton, *Science*, 2014, **344**, 186–189.
- 23 J. P. Gong, J. Katsuyama, T. Kurokawa and Y. Osada, *Adv. Mater.*, 2003, **15**, 1155–1158.
- 24 J. P. Gong, *Soft Matter*, 2010, **6**, 2583–2590.
- 25 B. D. Fairbanks, M. P. Schwartz, A. E. Halevi, C. R. Nuttelman, C. N. Bowman and K. S. Anseth, *Adv. Mater.*, 2008, **21**, 5005–5010.
- 26 S. C. Skaalure, PhD thesis, University of Colorado Boulder, 2014, pp. 99–113.
- 27 S. T. Gould, N. J. Darling and K. S. Anseth, *Acta Biomater.*, 2012, **8**, 3201–3209.

- 28 Y. C. Fung and P. Tong, *Classical and Computational Solid Mechanics*, 2001, p. 622.
- 29 U. Akalp, S. Chu, S. C. Skaalure, S. J. Bryant, A. Doostan and F. J. Vernerey, *Polymer*, 2015, **66**, 135–147.
- 30 P. J. Flory, *Principles of polymer chemistry*, Cornell University Press, 1953.
- 31 P. J. Flory and B. Erman, *Macromolecules*, 1982, **15**, 800e6.
- 32 M. Holmes and V. Mow, *J. Biomech.*, 1990, **23**(11), 1145e56.
- 33 M. Kwan, W. Lai and V. Mow, *J. Biomech.*, 1990, **23**(2), 145e55.
- 34 M. Rubinstein and R. H. Colby, *Polymer Physics*, Oxford University Press, 2003.
- 35 A. H. Aziz, J. Wahlquist, A. Sollner, V. Ferguson, F. DelRio and S. J. Bryant, *J. Mech. Behav. Biomed. Mater.*, 2017, **65**, 454–465.
- 36 S. Ahmed, T. Nakajima, T. Kurokawa, M. A. Haque and J. P. Gong, *Polymer*, 2013, **55**, 914–923.
- 37 C. Creton and M. Ciccotti, *Rep. Prog. Phys.*, 2016, **79**, 046601.